

Chemical Science

Accepted Manuscript



This is an *Accepted Manuscript*, which has been through the Royal Society of Chemistry peer review process and has been accepted for publication.

Accepted Manuscripts are published online shortly after acceptance, before technical editing, formatting and proof reading. Using this free service, authors can make their results available to the community, in citable form, before we publish the edited article. We will replace this *Accepted Manuscript* with the edited and formatted *Advance Article* as soon as it is available.

You can find more information about *Accepted Manuscripts* in the [Information for Authors](#).

Please note that technical editing may introduce minor changes to the text and/or graphics, which may alter content. The journal's standard [Terms & Conditions](#) and the [Ethical guidelines](#) still apply. In no event shall the Royal Society of Chemistry be held responsible for any errors or omissions in this *Accepted Manuscript* or any consequences arising from the use of any information it contains.

ARTICLE

Regioselective Thioacetylation of Chitosan End-Groups for Nanoparticle Gene Delivery Systems

Cite this: DOI: 10.1039/x0xx00000x

V. D. Pickenhahn^a, V. Darras^a, F. Dziopa^a, K. Binięcki^b, G. De Crescenzo^a, M. Lavertu^{a†} and M. D. Buschmann^{a†}Received 00th January 2012,
Accepted 00th January 2012

DOI: 10.1039/x0xx00000x

www.rsc.org/

Chitosan (CS) end-group chemistry is a conjugation strategy that has been minimally exploited in the literature to date. Although the open-chain form of the CS reducing extremity bears a reactive aldehyde moiety, the most common method to generate a reactive end group on CS is nitrous acid depolymerization, which produces a 2,5-anhydro-D-mannose unit (M-Unit) bearing also an aldehyde moiety. However, the availability of the latter might be low, since previous literature suggests that its hydrated and non-reactive form, namely the gem-diol form, is predominant in acidic aqueous conditions. Oxime-click chemistry has been used to react on such aldehydes with various degrees of success, but the use of a co-solvent and additional chemical reagents remain necessary to obtain the desired and stable covalent linkage. In this study, we have assessed the availability of the aldehyde reactive form on chitosan treated with nitrous acid. We have also assessed its reactivity towards thiol-bearing molecules in acidic conditions where CS amino groups are fully protonated and thus unreactive towards aldehyde. LC-MS and NMR spectroscopy methods (¹H and DOSY), confirmed the regioselective thioacetylation of the reactive aldehyde with conversion rates between 55-70% depending on the thiol molecule engaged. The stabilization of the hemithioacetal intermediates into the corresponding thioacetals was also found to be facilitated upon freeze-drying of the reaction medium. The PEGylation of CS M-Unit aldehyde by thioacetylation was also performed as a direct application of the proposed conjugation approach. CS-b-PEG2 block copolymers were successfully synthesized and were used to prepare block ionomer complexes with plasmid DNA, as revealed by their spherical morphology vs. the rod-like/globular/toroidal morphology observed for polyplexes prepared using native unmodified chitosan. This novel aqueous thiol-based conjugation strategy constitutes an alternative to the oxime-click pathway; it could be applicable to other polymers

Introduction

Chitosan (CS), a linear and cationic polysaccharide composed of D-glucosamine (GlcNH₂) and N-Acetyl-D-glucosamine (GlcNHAc) units, is derived from chitin by deacetylation. This non-toxic polyelectrolyte holds great interest due to its biocompatibility, biodegradability and mucoadhesive properties¹. Chitosan and its derivatives have been proposed for

applications including gene and drug delivery, tissue repair, water purification and cosmetics²⁻⁶. Two general approaches have been explored to chemically modify CS - lateral "graft" and "block" modifications. The former involves conjugation to CS lateral functional groups (amine or hydroxyl) while the latter relies on conjugation to CS end groups.

Several strategies for grafting onto CS amines (N-2-graft) have been proposed in the literature. For example, PEG and other graft-copolymers have been proposed to enhance CS solubility at physiological pH and increase colloidal stability of CS-based polyelectrolyte complexes^{7, 8}, while ligands for specific cell targeting^{9, 10} or fluorescent dyes^{11, 12} have also been grafted onto CS amines. However, lateral grafting can potentially compromise the ability of CS to bind nucleic acid and thus limit the stability and efficiency of chitosan/nucleic acid polyelectrolyte complexes for gene delivery applications. Indeed, lateral grafting can impede the ability of CS to electrostatically bind to negatively charged species by reducing its effective charge density and by potentially creating steric hindrance with bulky moieties⁴. Alternatively, the O-6 grafting has been proposed to overcome the charge density reduction issue, although grafting of a bulky moiety at this position is likely to create steric hindrance and hence limit complexation with oppositely charged polymers or molecules as well. Additionally, O-6 grafting is technically challenging as it necessitates protection-deprotection steps for the CS amine moieties¹³.

To overcome these limitations, CS block conjugation strategies (e.g., Branched CS^{14, 15}, PEGylation¹⁶, CS-PEI block-copolymer formation¹⁷, CS labeling¹⁸, etc.) have been recently proposed as a means to modify the CS properties without compromising its ability to bind oppositely charged macroions such as nucleic acids. Two different CS attachment sites have been explored to date: the first is formed after CS depolymerization by nitrous acid (HONO) where a 2,5-anhydro-D-mannose unit (M-Unit) is formed at the reducing end of the cleaved polymer (Figure 1 - reaction 1), while the second site is available on the open-chain form, present in trace amounts, of the CS reducing extremity (either GlcNH₂ or GlcNHAc units) and allows mutarotation between the alpha and beta anomers. These coupling strategies thus rely on the reaction of the aldehyde moiety with nucleophilic species. However, in both cases, the aldehyde moiety appears to be mostly present in its hydrated and unreactive form (Figure 1 - reaction 2), also referred to as the *geminal* or *gem*-diol form, under acidic aqueous conditions¹⁹⁻²¹.

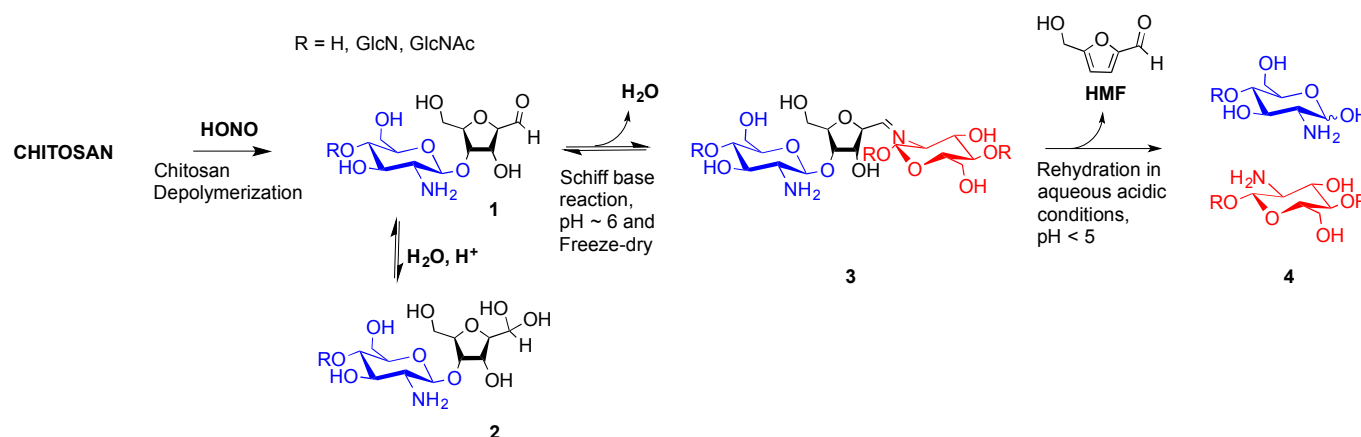


Figure 1. **Production of 2,5-anhydro-D-mannose unit (M-Unit) at the reducing end of chitosan by depolymerization in nitrous acid (HONO):** Chitosan depolymerization with nitrous acid (HONO) is a rapid, well-understood, and easily controlled method for producing chitosan harbouring a 2,5-anhydro-D-mannose unit (M-Unit) at the reducing end of the cleaved polymer²². A free aldehyde group (electrophile) is then potentially accessible (1) for reaction with nucleophilic moieties (e.g., CS amine groups, thiols, oxyamines, etc.). Tømmeraa *et al.* demonstrated that the M-Unit aldehyde also exists in its *gem*-diol hydrated form (2). The neutralization of CS and subsequent freeze-drying of the depolymerization medium induces a Schiff base formation between CS neutralized amines that react with the CS M-Unit aldehyde (3). The rehydration of the imino-adducts in acidic aqueous conditions cleaves the imino linkage between CS chains transforming the M-Unit into hydroxymethylfurfural (HMF) (4).

The amines of CS in their neutral form are strong nucleophiles that can react with the aldehyde of CS's reducing end (Figure 1 - reaction 3). Therefore block conjugation to the CS end group requires that the proportion of CS amines in their reactive form be minimized, for example by performing reactions at pH significantly lower than the chitosan pK_a, typically near 6.5. However, chitosan pK_a varies with both ionic strength and CS charge density and can reach values as low as about 5.5 at high charge density and in the absence of added salt²³. To date, all CS end-group conjugation reactions that have been implemented rely on oxime-click chemistry^{16, 18, 24, 25}. The

oxyamine moieties involved in these studies have a pK_a value around 5²⁶ and are therefore only slightly more reactive than CS amines in acidic aqueous conditions. Additionally, although the carbon-nitrogen double bond resulting from oxime-click chemistry is more hydrolytically stable than standard imino linkages²⁷, a conjugate stabilization by an external chemical reagent (e.g., hydrides) is necessary to stabilize the structure²⁸. Moreover, it appears that CS conjugations with such chemistry usually require a polar aprotic co-solvent addition such as acetonitrile, DMF or DMSO to improve reaction efficiency²⁹.

The only slightly higher reactivity of oxyamine moieties towards CS aldehyde as compared to CS amines, along with the necessity of an external chemical treatment to stabilize the products and the requirement of an organic co-solvent addition constitute limitations of the oxime-click pathway. These limitations could be overcome by a thiol-based chemistry. Indeed, thiol moieties are highly reactive towards double bonds as well as towards carbonyl groups in aqueous conditions at pH as low as 1 where CS amines are present only in the ionized and non-reactive form³⁰. Moreover many equilibrium measurements have demonstrated the ability of thiols to add to the carbonyl group more efficiently than other nucleophiles (e.g., hydroxyls or amines) in both acid- and base-catalyzed pathways³¹. Whereas amines produce Schiff base compounds (Figure 1 - reaction 3), thiols react with either aldehydes or ketones to produce hemithioacetals through a double equilibrium (Figure 2). It is worth mentioning that the reactive species is the dehydrated carbonyl compound so that dehydration and hemithioacetal formation represent the rate limiting steps of this pH dependent process^{30,32}.

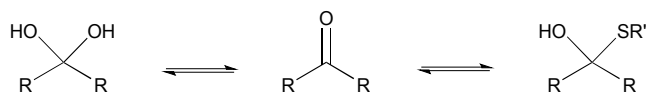


Figure 2. Schematic representation of the equilibria involved in thiol-carbonyl additions.

Indeed, acid catalyzed hemithioacetal formation takes place optimally below pH 3³⁰ and the final product is unstable under alkaline conditions, since the attack of hydroxide ions readily reverts the product to the starting reactants^{33,34}.

By analogy with Schiff base formation where amines and carbonyls react to give an imino linkage (Figure 1 – reaction 3) that needs to be stabilized by reduction, hemithioacetals can be stabilized by thioacetal formation via a second thiol nucleophilic attack (intra- or inter-molecular) associated with the release of water³⁵. This chemical process is widely used in

organic synthesis as a carbonyl group protection strategy; it is more conveniently performed in anhydrous organic solvent³⁶. To the best of our knowledge, such a strategy has not been implemented yet in aqueous conditions for polymer derivatization.

The main objectives of the present study were to determine which form of the aldehyde predominates on the CS end-group (i.e. hydrated vs. dehydrated form for a CS depolymerized using HONO) and to assess its reactivity towards thiol moieties in aqueous conditions. NMR spectroscopy experiments were performed in order to assess the availability of the CS aldehyde end-group after HONO depolymerization, since this issue has not been clearly addressed. The mechanism of stabilization of hemithioacetals by conversion to their corresponding thioacetals was also investigated by liquid chromatography - mass spectrometry (LC-MS) analysis of the products of the reaction between mannose and two small thiol-bearing molecules, namely 3-mercaptopropionic acid (MPA) and β -mercaptoethanol (BME). This process was then examined by reacting MPA and BME with a CS bearing an M-Unit end in aqueous conditions. The conjugation efficiency was determined by a combination of NMR and Ellman assays. Finally, the PEGylation of CS M-Unit aldehyde by thioacetylation was examined as a direct application of this conjugation strategy. Figure 3 summarizes the objectives and the hypotheses of our study. Of interest, although the unreactive hydrated *gem*-diol M-Unit aldehyde moieties are predominant in acidic aqueous conditions, the thiol species react preferentially with this M-Unit versus CS amines post-HONO depolymerization, therefore avoiding the M-Unit cleavage after rehydration of the freeze-dried product. The conjugation between the M-Unit and thiol species is followed by stabilization of the hemithioacetal intermediate into the corresponding thioacetal by a second thiol nucleophilic attack. By analogy with the Schiff base formation, freeze-drying can thus be implemented to favour the present reaction by water removal.

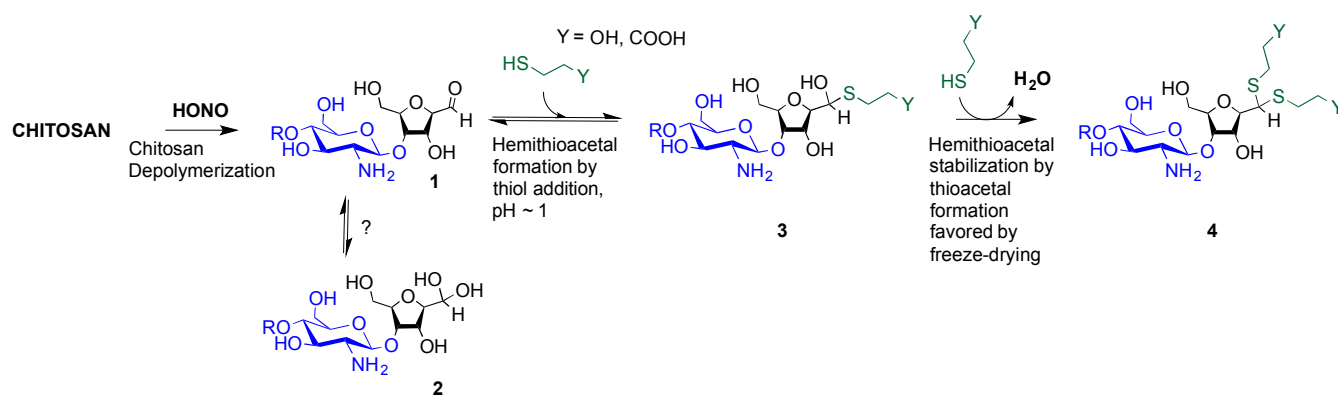


Figure 3. Thioacetal conjugation to the chitosan M-Unit formed post HONO depolymerization; The first objective of this study was to assess the availability of the reactive form of the unhydrated M-Unit aldehyde (2). Although there could be a strong displacement of the equilibrium towards the unreactive aldehyde-hydrated or *gem*-diol form in water, we hypothesized that efficient nucleophilic conjugation to the M-Unit was possible in acidic aqueous conditions. The second objective was to assess the M-Unit reactivity towards thiol moieties in aqueous conditions. The proposed reaction pathways between CS end-groups and thiols include the M-Unit CS aldehyde reacting directly with a thiol-bearing model molecule (β -mercaptoethanol and 3-mercaptopropionic acid, BME and MPA respectively) to form a

hemithioacetal intermediate (3) through a pH dependent equilibrium. By analogy with Schiff base formation where the equilibrium displacement occurs by water removal, the hemithioacetal can be stabilized into the corresponding thioacetal (4) by freeze-drying.

Materials and Methods

Each chemical reaction was performed on at least three independent occasions ($N = 3$), in Ar degassed ddH₂O and fresh reactants to minimize disulfide bond formation.

Reagents, Materials

Chitosan with a degree of deacetylation (DDA) of 91.7%, $M_n = 193$ kg.mol⁻¹ (PDI=1.256) and 99.5%, $M_n = 0.8$ kg.mol⁻¹ (PDI=1.245) was provided by Marinard Biotech Inc. Deuterium oxide (Cat #151882), Deuterium chloride 35 wt. % in deuterium oxide (Cat #543047), Sodium nitrite (Cat #431605), Hydrochloric acid standard solution - 1.0 N in H₂O (Cat #31,894-9), Hydrochloric acid 37% (Cat #320331), Sodium hydroxide solution 1.0M (Cat #319511), Sodium acetate (Cat #241245), DTNB (5,5'-dithiobis-(2-nitrobenzoic acid)) (Cat #D8130), GlcNH₂ D-(+)-Glucosamine hydrochloride 99% (Cat #C-1276), MPA (3-Mercaptopropionic acid) $\geq 99\%$ (Cat #63768), BME (β -Mercaptoethanol) (Cat #M6250), Sodium acetate trihydrate BioXtra (Cat #S7670), Dowex® 50WX8-100 [H⁺] (Cat #217506), Dowex® 1X8-50 [Cl⁻] (Cat #217417) and Sodium azide (Cat #S2002) were purchased from Sigma-Aldrich. UltraPure™ TRIS (Cat #15504-020), Glacial acetic acid (Cat #351271-212) and Spectra/Por®6 dialysis membrane (MWCO=1000 Da, Cat #132640) were purchased from Life Technologies, Fisher Scientific and Spectrum Labs respectively. mPEG-SH 2 kDa and the plasmid DNA (pDNA) pEGFPLuc were purchased from JenKem Technology USA and from Clontech Laboratories, respectively.

Aldehyde availability

Chitosan depolymerization using deuterated species for direct ¹H NMR measurements²². The depolymerization reaction was performed in deuterated solvent for direct M-Unit CS aldehyde detection by ¹H NMR spectroscopy without further processing post-reaction. Chitosan with 92% DDA and $M_n = 200$ kg.mol⁻¹ (CS 92-200) was depolymerized using nitrous acid in deuterated solvent to achieve a specific number-average molar mass (M_n) target of 1 kg.mol⁻¹ (CS 92-1). These short CS chains were used to facilitate the detection and the quantification of aldehyde end groups. Chitosan (202.5 mg) was dissolved in 37.9 mL D₂O and 170 μ L of DCI 35% (w/w) at 50°C. Then 2.435 mL of fresh sodium nitrite solution (10 mg.mL⁻¹ in D₂O) was added to the dissolved CS to reach 0.5% (w/v) chitosan concentration. These conditions correspond to a GlcNH₂:HONO molar ratio of 3. The mixture was stirred for 3h at 50°C. The pD ($pD = pH + 0.4$)³⁷ of the depolymerization medium was ca. 1.9 at the end of the reaction.

¹H NMR (Sup. info. S1) (500 MHz, D₂O/DCI, 70°C, $n_s = 2000$, $d_1 = 6s$, acquisition time=2s) δ 2.06 (s, 1.38H, NHAc), 3.13-3.19 (br, 4.5H, H2D), 3.49-3.51 (br, 1H, H2A), 3.73-3.95 (m, 27H,

H3-H6), 4.12-4.13 (q, $J = 5.1$ Hz, 1H, H5M), 4.22 (t, $J = 3.9$ Hz, 1H, H4M), 4.44 (t, $J = 3.9$ Hz, 1H, H3M), 4.58 (br, 0.5H, H1A), 4.79-4.88 (m, 4.5H, H1D), 5.09 (d, $J = 5.3$ Hz, 0.98H, H1M Gem-diol).

SEC-MALLS : $M_n = 823 (\pm 41)$ g.mol⁻¹ ; $M_w = 1024 (\pm 28)$ g.mol⁻¹ ; PDI = 1.245 (± 0.027).

Thiol reactivity towards M-Unit CS aldehyde

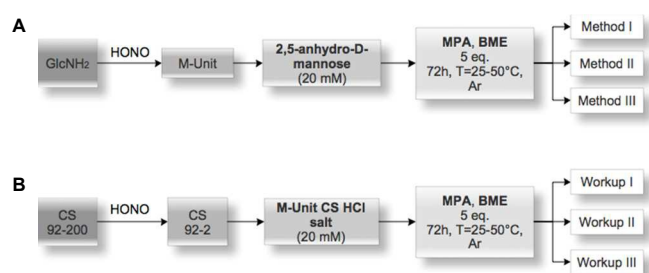


Figure 4. Experimental Design Flowchart. A) Mechanistic studies. Glucosamine (GlcNH₂) was treated with nitrous acid to form the 2,5-anhydro-D-mannose (M-Unit) that was reacted with 2 thiol-bearing molecules (β -mercaptoethanol and 3-mercaptopropionic acid, BME and MPA, respectively). The reaction products were treated using one of 3 methods, i.e. Method I: Direct LC-MS analyses to determine to which extent thioacetal formation occurs *in situ*; Method II: Freeze-drying (FD) + LC-MS analyses to assess the effect of FD on the thioacetal proportion and to ascertain that no by-products appear post FD; Method III: Acetate buffer pH 4 + FD + LC-MS analyses to determine the effect of an increase in pH prior to FD (this pH increase was included here to prevent any CS acid hydrolysis that could occur when Method II, i.e. FD at pH 1, would be transposed to the polymer). B) Chitosan M-Unit reactivity. CS 92-200 was depolymerized with nitrous acid to produce CS 92-2 HCl salt bearing the M-Unit at the cleaved end of the polymer. M-Unit CS 92-2 HCl salt were reacted with MPA and BME and the reaction products treated with one of 3 workups: Workup I: Dialysis vs. HCl 1mM solution + FD to remove all thiol model excess and to determine the *in situ* thioacetal formation rate; Workup II: FD + Dialysis vs. HCl 1mM solution + FD to determine the effect of FD on the functionalization rate; Workup III: Acetate buffer pH 4 + FD + Dialysis vs. HCl 1mM solution + FD to determine the effect of an increase in pH prior to FD on the functionalization rate (this pH increase was included to prevent any CS acid hydrolysis that could occur during FD at pH 1 in Workup II). The degree of functionalization of the CS conjugates was determined by ¹H NMR, whereas covalent conjugation was assessed by DOSY NMR experiments and Ellman assays in order to rule out the possibility of a simple physical mixture of reagents.

Mechanistic evaluation of chitosan thioacetylation by mass spectrometry (Figure 4-A). The CS terminal end-group (2,5-anhydro-D-mannose) formed after HONO depolymerization was derivatized with thiol-bearing model molecules (BME and MPA). Since the expected products have similar structures, their sensitivity to ionization should be equivalent. These derivatized M-Unit products were analyzed in a semi-quantitative way by comparing the chromatogram integration peaks of specific m/z values corresponding to both proton ($[M+H]^+$) and sodium adducts ($[M+Na]^+$) within the same run.

2,5-anhydro-D-mannose (M-Unit) synthesis.

2,5-anhydro-D-mannose was synthesized according to Claustre *et al.*³⁸. Briefly, GlcNH₂.HCl (5 mmol, 1 g) was dissolved in 25 mL degassed ddH₂O and was allowed to stir overnight at room temperature. The colorless reaction medium was cooled down to 0°C and NaNO₂ (12.5 mmol, 862 mg) was added. Dowex® 50WX8-100 [H⁺] resin (42.5 mmol, 8.85 g dried, 25 mL) was added slowly under stirring and the heterogeneous mixture stirred for 4h at 0-5°C. The H⁺ resin was removed by filtration and the filtrate was neutralized with Dowex® 1X8-50 [CO₃²⁻] resin (60 mmol, 17.14 g dried, 50 mL), flash-frozen and freeze-dried to give the expected yellowish solid with 85% yield.

¹H NMR (500 MHz, D₂O, 25°C, ns=64, d1=6s, acquisition time=2s) δ 3.36-3.40 (m, 2H, H6), 3.91-3.95 (m, 2H, H2 & H5), 4.05-4.08 (t, J=5.6 Hz, 1H, H4), 4.18-4.21 (t, J=5.8 Hz, 1H, H3), 5.09-5.10 (d, J=5.4Hz, 0.88H, H1 Gem-diol), 8.46 (s, 0.12H, H1 Aldehyde).

MS (ESI⁺): [M+H⁺] = 163.0625; [M+Na⁺] = 185.0460 (Expected: [M+H⁺] = 163.0601; [M+Na⁺] = 185.0420)

2,5-anhydro-D-mannose (M-Unit) conjugation with thiol-bearing molecules

The synthesized 2,5-anhydro-D-mannose M-Unit (0.1 mmol, 16.2 mg) was dissolved in 5 mL degassed ddH₂O. The pH of the solution was adjusted to 1 with 3M HCl solution prior to the addition of the thiol-bearing molecule (0.5 mmol, 53.2 μL for MPA and 35.1 μL for BME). The pH was readjusted to 1 with 3M HCl solution. The reaction mixture was stirred for 72h at 25°C, under Ar atmosphere and covered with aluminum foil. The reaction mixture turned clear pink-orange after 72h and was split into 3 parts (Methods I, II and III): the first was dedicated to the direct LC-MS analysis of the reaction medium in order to determine the thioacetal proportion in resulting conjugates that formed *in situ*; the second one was directly flash-frozen and then freeze-dried prior to LC-MS analyses to assess the effect of FD on the thioacetal proportion in resulting conjugates and to ascertain that no by-products appear post FD, whereas the third was treated with 1M acetate buffer pH 4 before flash-freezing and freeze-drying in order to determine by LC-MS the effect of an increase in pH on the resulting conjugates. It is worth mentioning that Method III was included to prevent any CS acid hydrolysis that could occur when Method II, i.e. FD at pH 1, would be transposed to the polymer.

Characterization: Mass Spectrometry

Liquid chromatography - mass spectrometry (LC-MS) data were acquired on an Agilent 6224 LC-TOF mass spectrometer in positive electrospray ion mode, coupled to an Agilent 1260 series liquid chromatography system (Agilent Technologies). Mass Hunter B.06 software (Agilent Technologies) was used to process data. Separations were carried out at 50°C on a XSELECT CSH™ C18 column (4.6 x 100mm, 5μm particles) from Waters. The auto-sampler was maintained at 15°C to avoid sample degradation. The eluents consisted of 0.1% formic acid in water (eluent A) and 0.1% formic acid in acetonitrile (eluent B). The initial mobile phase contained 1% eluent B and was held for 3 min. Eluent B content was

increased from 1 % to 20 % from 3 to 5 min then from 20 % to 80 % from 5 to 7 min. The system returned to the initial conditions at 7.2 min and was held constant for up to 15 min to allow column equilibration. The injection volume was 1-3 μL. A needle wash solution containing methanol:water (60:40 v/v) was used after each injection to reduce carry-over. Mass spectra were acquired for m/z ranging from 50 to 1200.

Liquid chromatography coupled to tandem mass spectrometry (LC-MS/MS) experiments were performed on a Thermo Scientific Quantum Ultra triple quadrupole mass spectrometer operated in positive electrospray ion mode, equipped with a Thermo Scientific Surveyor liquid chromatography system. Xcalibur software (Thermo Scientific) was used to process data. Separations were carried out on a XSELECT CSH™ C18 column (4.6 x 100mm, 5μm particles) from Waters operated under the same chromatographic gradients as those described above. MS/MS spectra were acquired on m/z values for protonated [M+H]⁺ and sodium adduct [M+Na]⁺ species of targeted compounds.

Chitosan end-group reactivity (Figure 4-B). Chitosan with 92% DDA and Mn = 200 kg.mol⁻¹ (CS 92-200) was depolymerized with nitrous acid (HONO) to a final molar mass of 2 kg.mol⁻¹ (CS 92-2). The final product was kept in its hydrochloride salt form by dialysis vs. HCl 1mM solution and freeze-drying to minimize CS amines reacting with the M-Unit. This low 2kDa molar mass was chosen in order to facilitate the elimination by dialysis of unreacted model thiols from the reaction mixture. The CS hydrochloride salt, carrying the 2,5-anhydro-D-mannose unit (M-Unit), was allowed to react at pH 1 with the two thiol models: 3-mercaptopropionic acid (MPA) and β-mercaptoethanol (BME). Each reaction was allowed to stir for 72h, at two different temperatures (25 and 50°C) under Ar atmosphere and were treated using three different workups: Workup I) Dialysis vs. HCl 1mM solution followed by freeze-dry (FD) to remove all thiol-bearing molecule excess and to determine the *in situ* thioacetal functionalization degree); Workup II) Direct FD, dialysis vs. HCl 1mM solution and a final FD to determine the effect of FD on the functionalization degree; Workup III) 1M Acetate buffer pH 4 addition to protect CS from acid hydrolysis during FD at pH 1, dialysis vs. HCl 1mM solution and another FD to assess the effect of an increase in pH prior to FD on the functionalization rate. All conditions implemented are summarized in Figure 4. Each final product was characterized by ¹H NMR, Diffusion Ordered Spectroscopy (DOSY) (5 mg.mL⁻¹ with 2% DCl in D₂O), SEC-MALLS (1 mg.mL⁻¹ in duplicates) and free thiol content was determined by Ellman assay (before and after Zn/HCl treatment to reduce any disulfide bond³⁹ that would not have been detected by the Ellman method). The following protocols describe the CS preparation as well as examples of the conjugation reactions performed in this study.

M-Unit CS 92-2 HCl salt synthesis

Chitosan was depolymerized using nitrous acid to achieve specific number-average molar mass targets (Mn) of 2 kg.mol⁻¹

¹. For depolymerization, chitosan (1 g) was dissolved in 184.5 mL ddH₂O and 9.54 mL HCl 1N solution at 50°C. Then 5.975 mL of fresh sodium nitrite solution (10 mg.mL⁻¹ in ddH₂O obtained by solubilization of 76.5 mg NaNO₂ in 7.65 mL ddH₂O) were added to the completely dissolved CS to reach 0.5% (w/v) chitosan concentration. These conditions correspond to a GlcNH₂:HONO molar ratio of 6. The viscous colorless mixture was stirred for 3h at 50°C. The reaction medium was then dialyzed 5x against 4L of an aqueous solution of HCl at pH 3 (HCl 1mM solution) over 2 days. The resulting colorless solution was flash-frozen with liquid nitrogen and freeze-dried over 3 days to give the desired white powder with 60-70% yield.

¹H NMR (500 MHz, D₂O, 70°C, ns=64, d1=6s, acquisition time=2s) δ 2.06 (s, 3.16H, NHAc), 3.14-3.21 (br, 13H, H2D), 3.51-3.56 (br, 1H, H2A), 3.68-3.95 (m, 70H, H3-H6), 4.12 (br, 1H, H5M), 4.21-4.31 (br, 1H, H4M), 4.43 (br, 1H, H3M), 4.61 (br, 1H, H1A), 4.87-4.89 (m, 13H, H1D), 5.08 (d, J=5.0 Hz, 1H, H1M Gem-diol).

SEC-MALLS: Mn = 2342 (± 11) g.mol⁻¹; Mw = 3117 (± 4) g.mol⁻¹; PDI = 1.332 (± 0.008)

M-Unit CS 92-2 HCl salt conjugation with thiol-bearing molecules

CS 92-2 HCl salt (0.035 mmol, 70 mg) and thiol-bearing model molecules (0.175 mmol, 25.4 μL for MPA, 12.3 μL for BME) were solubilized in 1.73 mL degassed ddH₂O. The pH of the reaction medium was adjusted to 1 with 3M HCl. The reaction medium was stirred for 72h at either 25 or 50°C under Ar atmosphere. The resultant colorless liquid was directly flash-frozen with liquid nitrogen and then freeze-dried over 3 days. The freeze-dried white solid was solubilized in 5 mL ddH₂O and dialyzed 5x against 2L HCl 1mM solution to remove unreacted thiols. The colorless solution was flash frozen and freeze-dried to give the expected white solid with typically 70-80% yield.

Addition of BME (Sup. info. S2): ¹H NMR (500 MHz, D₂O/DCI, 70°C, ns=64, d1=6s, acquisition time=2s) δ 2.06 (s, 5.89H, NHAc), 2.91-2.95 (br, 2.78H, BME-CH₂S), 3.17-3.21 (br, 20H, H2D), 3.51-3.53 (br, 1H, H2A), 3.69-3.95 (m, 105H, H3-H6), 4.12-4.14 (br, 1H, H5M), 4.24-4.25 (br, 1H, H4M), 4.57-4.59 (br, 1H, H3M), 4.61-4.62 (br, 1H, H1A), 4.91-4.92 (m, 20H, H1D), 5.08-5.09 (d, J=5.0 Hz, 0.30H, H1M Gem-diol).

SEC-MALLS: Mn = 3177 (± 57) g.mol⁻¹; Mw = 3680 (± 66) g.mol⁻¹; PDI = 1.160 (± 0.003)

Addition of MPA (Sup. info. S3): ¹H NMR (500 MHz, D₂O/DCI, 70°C, ns=64, d1=6s, acquisition time=2s) δ 2.06 (s, 4.18H, NHAc), 2.74-2.77 (t, J=7.1 Hz, 2.33H, MPA-CH₂-CO), 2.97-3.01 (q, J=6.8 Hz, 1.78H, MPA-CH₂S), 3.15-3.24 (br, 17H, H2D), 3.51-3.56 (br, 1H, H2A), 3.69-3.95 (m, 91H, H3-H6), 4.11 (br, 1H, H5M), 4.21-4.23 (br, 1H, H4M), 4.55 (br, 1H, H3M), 4.62 (br, 1H, H1A), 4.87-4.92 (m, 17H, H1D), 5.08 (d, J=5.0 Hz, 0.47H, H1M Gem-diol).

SEC-MALLS: Mn = 3053 (± 81) g.mol⁻¹; Mw = 3564 (± 48) g.mol⁻¹; PDI = 1.182 (± 0.016)

Ellman Assays

Thiol-derivatized CSs were analyzed by the Ellman assay to assess the presence of free thiols within the products. Ellman stock solutions (50 mM sodium acetate, 2 mM DTNB) were prepared by dissolving 39.7 mg of Ellman reagent and 205.1 mg of sodium acetate in 50 mL double deionized water (ddH₂O). Tris 1M dilution buffer was prepared dissolving 6.1 g of Tris in 50 mL ddH₂O and adjusting the pH to 8.0 using HCl 1.0 N standard solution. Thiol concentrations were measured in triplicate by mixing 50 μL of Ellman stock solution with 100 μL of Tris dilution buffer and 10 μL of sample solution. After 15 min the mixture was diluted by the addition of 840 μL of ddH₂O and the absorbance at 412 nm read using a microplate reader Tecan Infinite® M200. Thiol concentrations were calculated from a standard curve prepared using either MPA or BME and measurements were performed in triplicates in a 96 well plate using 150 μL sample volumes. The CS used as starting material was dissolved at the appropriate concentration for each sample and used as a blank. Both NaOH and Zn/HCl treatments of the CS adduct solutions were implemented on separate samples to determine the presence of hemithioacetal intermediates and any disulfide bond formation within the final product by the Ellman assay, respectively. Concentrated 1M NaOH and 1M HCl solutions were used to minimize changes in CS concentration. After 45-60 min constant agitation of the reaction media, Ellman assays were performed using 10 μL of alkali sample solution for NaOH treatment. Zn/HCl treated samples were obtained by adding few μL of 1M HCl (to reach pH 1) and 5 equivalents of Zn dust per CS; the supernatants were analyzed after centrifugation (1000g for 1 min).

Characterization: NMR and SEC-MALLS

The deacetylation degree (DDA) of chitosan was determined by ¹H NMR spectroscopy as previously described⁴⁰ using a Bruker Avance 500 spectrometer equipped with a Bruker 5 mm BBFO probe. Cross-polarization magic-angle spinning (CPMAS) and Bloch-decay (BD) ¹³C NMR spectra were collected on a Bruker Avance 600 instrument equipped with a Bruker 4mm BL4 CPMAS probe and samples were spun at the magic angle (54.7°) at a rate of 10-12 kHz. Diffusion ordered spectroscopy experiments (DOSY) were conducted on a Bruker II 400 equipped with a Bruker diff30 probe, using 32 gradients between 11.2 and 358.4 gauss.cm⁻¹ with a gradient pulse (δ) of 1 ms, a diffusion time (Δ) of 60 ms.

Molar mass of starting 92% DDA chitosan was determined by size-exclusion chromatography (SEC) as previously described⁴¹. Measurements were acquired on a gel permeation chromatography system equipped with LC-20AD isocratic pump, SIL-20AC HT autosampler, CTO-20AC oven (Shimadzu). This setup was coupled to the following detectors: Dawn HELEOS II multiangle laser light scattering, Viscostar II viscosimeter and Optilab rEX interferometric refractometer (Wyatt Technology Co.). The starting materials were eluted

through two Shodex OHPak columns (SB-806M HQ and SB-805 HQ) connected in series with a mobile phase composed of 0.15M acetic acid, 0.1M sodium acetate, 0.4mM sodium azide, 0.1M NaCl, pH 4.5⁴². A dn/dc value of 0.214 (DDA=92%) was used and the number and weight average molar masses (M_n and M_w) of the CS starting materials were found to be 193 kg.mol⁻¹ and 242.5 kg.mol⁻¹ respectively.

Modified CS (depolymerized CS and thiol coupled CSs) were analyzed in SEC using the same conditions but with columns SB-806M HQ and SB-803 HQ that are more suitable for the analysis of low molecular weight chitosans.

Quantitation of CS derivatization efficiency: Functionalization degree (F) calculations

The functionalization degrees (F) of each conjugation were calculated according to the following equations:

$$F = \frac{\frac{1}{\alpha} \sum \int H_{\text{Thiol peaks}}}{\frac{1}{\beta} \sum \int H_{\text{M-Unit peaks}}} \times 100 \quad \text{Equation 1}$$

Where $H_{\text{Thiol peaks}}$ refers to the well-defined proton peaks of the thiol-bearing molecule conjugated to CS and $H_{\text{M-Unit peaks}}$ corresponds to the well-defined M-Unit characteristic proton peaks. Both integrations in Equation 1 are normalized to the number of protons used for the calculation, namely α and β for the thiol-bearing molecule and M-Unit, respectively.

According to the mechanistic studies on the M-Unit model presented below, the hemithioacetal intermediate is fully stabilized into the corresponding thioacetal (as shown in Figure 3 – reaction 4 and Figure 5) after freeze-drying of the reaction mixture in acidic conditions, thus two thiol-bearing molecules per M-Unit CS salt were considered for the calculation of the functionalization degree (F). For MPA adducts, two well-defined peaks corresponding to -CH₂-S- and -CH₂-CO- protons (i.e. 8 protons) appear on the NMR spectra. However, for BME adducts, only the -CH₂-S- peak is visible on the spectra, in agreement with NMR spectrum simulation⁴³ that predicts that -CH₂-CO- peak is hidden by the CS H3-H6 broad peaks⁴⁰. Thus, α values of 4 and 8 in Equation 1 were used for BME and MPA, respectively. For the M-Unit, the well-defined peaks corresponding to H₄M and H₅M protons were used for integration and a β value of 2 was thus used in Equation 1. From the above considerations, Equation 1 can be rewritten as Equation 2 and Equation 3 for BME and MPA conjugates, respectively:

$$F_{\text{BME}} = \frac{\frac{1}{4} \int H_{\text{CH}_2\text{-S}}}{\frac{1}{2} \int (H_{4\text{M}} + H_{5\text{M}})} \times 100 \quad \text{Equation 2}$$

$$F_{\text{MPA}} = \frac{\frac{1}{8} \left(\int H_{\text{CH}_2\text{-S}} + \int H_{\text{CH}_2\text{-CO}} \right)}{\frac{1}{2} \int (H_{4\text{M}} + H_{5\text{M}})} \times 100 \quad \text{Equation 3}$$

Where the protons used for integration are defined in Figure 5, for purified BME and MPA chitosan adducts.

Similarly, CS PEGylation efficiency (F_{PEG}) was also calculated by adapting Equation 1 with the PEG characteristic peak integrations:

$$F_{\text{PEG}} = \frac{\frac{1}{6} \int H_{\text{PEG-OCH}_3}}{\frac{1}{2} \int (H_{4\text{M}} + H_{5\text{M}})} \times 100 \quad \text{Equation 4}$$

where $H_{\text{PEG-OCH}_3}$ refers to the well-defined methyl protons (3 H) peaks located at the end of the PEG chain ($\alpha=6$ as there are 2 PEG chains per CS).

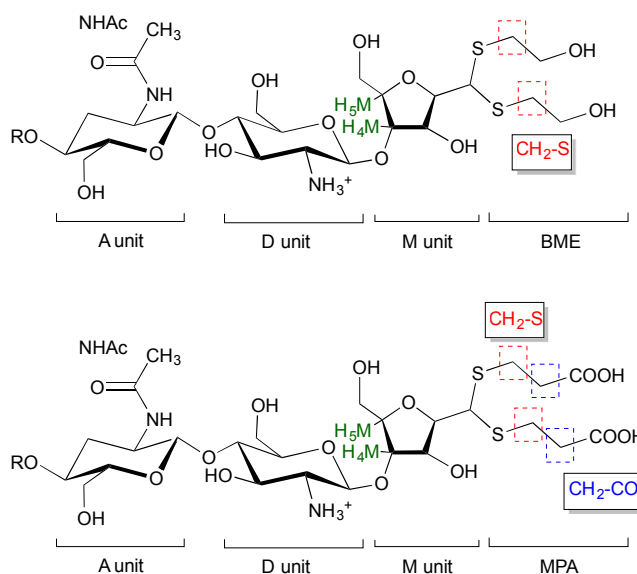


Figure 5. Structure of BME (top) and MPA (bottom) chitosan adducts. The protons corresponding to the ¹H NMR peaks used for the calculations of the functionalization degree in Equation 2 and Equation 3 are highlighted.

CS-b-PEG₂ block-copolymer

CS-b-PEG₂ block-copolymer formation. In order to reduce any mPEG-SS-PEG_m disulfide bonds, mPEG-SH (2kDa, $m = 200$ mg, 0.1 mmol) was solubilized in 2 mL Zn/HCl pH 1 solution ($m(\text{Zn}) = 9.8$ mg, 0.15 mmol) and the mPEG-SH solution stirred for 1h. The clear colorless reduction medium was centrifuged at 1000g for 2min prior to CS conjugation. M-Unit CS 92-10 HCl salt ($m = 100$ mg, 0.01 mmol, 5 mM aldehyde) was added to the reduced mPEG-SH solution and the pH of the reaction medium was adjusted to 1 with HCl 3N solution. The reaction medium was stirred for 72h at 50°C, under Ar atmosphere. At the end of the reaction, the reaction medium was flash-frozen and freeze-dried. Unreacted mPEG-SH was discarded by reprecipitation in 5 x 45 mL CH₂Cl₂. The remaining white pellet was dried under reduced pressure overnight.

¹H NMR (Figure 8) (500 MHz, D₂O, 70°C, ns=64, d1=6s, acquisition time=2s) δ 2.06 (s, 11H, NHAc), 3.14-3.22 (br, 46H, H2D), 3.37 (s, 3.67H, PEG-OCH₃), 3.51-3.56 (br, 3H, H2A), 3.69 (s, 181H, PEG Chain -O-CH₂-CH₂), 3.75-3.95 (m, 238H, H3-H6), 4.12-4.14 (br, 1H, H5M), 4.21-4.23 (br, 1H,

H4M), 4.61 (br, 3H, H1A), 4.88-4.90 (m, 46H, H1D), 5.08 (d, J=5.0 Hz, 0.49H, H1M *Gem*-diol).

CS-b-PEG₂ and CS/pDNA polyplexes formation. Polyplexes were prepared as previously described⁴⁴. Briefly: CS-b-PEG₂ and depolymerized unmodified chitosan (CS 10 kDa with 92.5% DDA) stock solutions were prepared by dissolution at 0.5% (w/v) in hydrochloric acid using a glucosamine:HCl ratio of 1:1. Polymer stock solutions were diluted with ddH₂O to reach the amine to phosphate ratio of 3.7 (N/P=3.7) when equal volumes of chitosan and pDNA (100 µg.mL⁻¹) solutions would be mixed. Both CS-b-PEG₂/pDNA and CS/pDNA polyplexes were prepared at room temperature, by adding 100 µL of the diluted polymer solution to 100 µL of the pDNA solution followed by immediate mixing by pipetting up and down. The polyplexes were analyzed for their size and morphology by dynamic light scattering (DLS) and environmental scanning electron microscopy (ESEM) 1h after their formation.

Polyplexes characterization. Average diameters (Z-Average) of chitosan/pDNA and CS-b-PEG₂/pDNA polyplexes were determined by dynamic light scattering (DLS) at an angle of 173° at 25°C, using a Malvern Zetasizer Nano ZS (Malvern, Worcestershire, UK). Samples (N = 2) were measured in triplicates using the viscosity of pure water in calculations. Environmental scanning electron microscopy (ESEM) imaging of the polyplexes were performed as previously described⁴⁵ on an environmental scanning electron microscope, Quanta 200 FEG (FEI Company Hillsboro, OR) operated in high vacuum mode with accelerating voltage = 20.0 kV; spot size = 3 and working distance = 5mm.

Results and Discussion

Aldehyde availability

Since hemithioacetal formation requires the dehydrated aldehyde as reactive species (referred to aldehyde in this manuscript), the CS aldehyde availability was assessed by NMR spectroscopy.

Chitosan 2,5-anhydro-D-mannose unit (M-Unit) - Gem-diol ubiquity. Raw CS was depolymerized using HONO to a final molar mass of 1 kg.mol⁻¹ (CS 92-1). This low Mn was chosen to increase the concentration of aldehyde moieties, facilitating their detection by ¹H NMR spectroscopy. The use of deuterated solvent for the depolymerization reaction in this study allowed direct NMR analysis of the reaction mixture (Sup. info. S1). In ¹H NMR spectrum, no aldehyde group was observed either at 9-9.5 ppm (the expected aldehyde proton chemical shift), nor at 8.5 ppm (for the M-Unit model) despite the use of a large number of scans (2000). However its hydrated form, the gem-diol peak at 5.09 ppm was omnipresent within the reaction medium. It is worth mentioning that the absence of the dehydrated form in the NMR spectrum is not due to a fast exchange between hydrated and dehydrated forms since both forms were detected for the 2,5-anhydro-D-mannose (M-Unit).

Equilibrium is strongly displaced towards the gem-diol form for the M-Unit CS. The hydrated form of the aldehyde was the only form detected in each liquid NMR analysis, either at 25°C (data not shown) or 70°C (Sup. info. S1). It is worth mentioning that these analyses were performed in D₂O and/or D₂O/DCI, which are favorable conditions for the hydrated form or *gem*-diol formation⁴⁶. Some authors also reported an increase in the acetaldehyde carbonyl hydration equilibrium constant ($K_{\text{hyd}} = [\textit{Gem-diol}]/[\text{Aldehyde}]$) from 0.85 to 0.99 when experiments are performed in ddH₂O and D₂O respectively, showing that the equilibrium can be displaced towards the formation of *Gem*-diol in deuterated solvents^{30,46}. In order to eliminate the contribution of the aqueous solvent on this equilibrium and to favor a displacement towards the aldehyde or unhydrated form of CS end unit, 1 kg.mol⁻¹ M-Unit CS HCl salt was analyzed by solid-state NMR (CP-MAS). Fully deacetylated CS (CS 99-1) was preferred to the CS 92-1 to avoid any confusion between the carbonyl chemical shift of the acetyl peak and the aldehyde peak. The same sample was analyzed at 2 different frequencies (10 kHz and 12 kHz) to detect the eventual presence of harmonics within the spectrum. All peaks corresponded to chemical moieties attributed according to Heux *et al.*⁴⁷ (data not shown). The CS salt did not form any Schiff base product, as expected (since protonated amines are not nucleophilic), however no aldehyde peak was detected in these spectra.

It has been reported that hydration of an aldehyde in the gas-phase can be observed at relative humidity (RH%) level as low as 5%⁴⁸. The relative humidity of the laboratory where the experiments were performed was between 20-50%, and it could be that all aldehyde groups were transformed into *gem*-diols during the sample transfer and preparation. To eliminate the exposure to air humidity that might favor this formation of the *gem*-diol, an inert atmosphere solid state NMR experiment was implemented on an extra-dried CS 99-1 salt (freeze-dried over 3 days and then dried using Speed-Vac Plus Centrifuge at 60°C, overnight under reduced pressure). Sample preparation was performed within an Ar glove box to verify if air humidity transforms the CS terminal aldehyde into its corresponding hydrate. The solid state NMR analysis was conducted under inert atmosphere as well (constant N₂ flow). Neither the aldehyde peak (expected around 190 ppm)⁴⁹, nor the *gem*-diol peak (expected around 90 ppm)²⁰ were visible on the spectrum. It is worth mentioning that the expected chemical shift of *gem*-diol falls within the range of chemical shifts corresponding to C3-C5 peaks and the former is most probably hidden by the latter (Sup. info. S4). In order to confirm that the absence of *gem* diol in the spectrum was not due to an unexpected side reaction occurring in the preparation of chitosan sample, the dried sample was subsequently dissolved in D₂O and analyzed by standard ¹H NMR. This analysis revealed that the hydrated aldehyde form was present at the expected quantitative proportion, as established from CS Mn and DDA (data not shown).

H-bonding could stabilize the M-Unit CS *gem*-diol. Although for most aldehydes and ketones the hydrates are generally less

stable than their respective parent⁴⁶, their equilibrium can be displaced towards the gem-diol form by making the carbonyl more electropositive. Thus, the gem-diol form can predominate when the aldehyde is located close to a functional group allowing a negative inductive effect. For CS, some suitable electron-withdrawing substituents, such as hydroxyl and hemiacetal substituents might create a weak negative inductive effect, thereby increasing slightly the δ^+ charge on the carbon of the carbonyl and favouring water nucleophilic attack. Since CS offers significantly more H-bond donors than 2,5-anhydro-D-mannose, intermolecular H-bonding may be responsible for the strong predominance of the gem-diol form⁵⁰. This hypothesis was confirmed with the ¹H NMR analysis of the synthesized 2,5-anhydro-D-mannose that presents a detectable proportion of the aldehyde in ¹H NMR spectroscopy (around 10% of the aldehyde form, data not shown). The NMR experiments described above suggest that the M-Unit CS aldehyde is only present in trace amounts since only the gem-diol form was detected. Nonetheless these trace amounts are reactive enough to be engaged with nucleophiles such as CS amines (Schiff base formation) or more particularly with thiol moieties (Figure 1, Figure 3).

Mechanisms of conjugation of 2,5-anhydro-D-mannose (M-Unit) and thiol-bearing molecules

The reactivity of aldehydes toward thiols in aqueous conditions was assessed semi-quantitatively by LC-MS using the 2,5-anhydro-D-mannose as an aldehyde model.

Expected products of thiol conjugation to aldehydes include hemithioacetal, thioacetal, oxathiolane and α, β -unsaturated sulfide intermediate. The expected products of all conjugations implemented with thiol-bearing molecules (MPA and BME) include hemithioacetal, thioacetal, oxathiolane and α, β -unsaturated sulfide intermediate (Figure 6). The first thiol attack on the aldehyde forms a hemithioacetal intermediate (*A*), which is in equilibrium with its corresponding protonated hemimercaptal form (oxonium) via a proton transfer. This structure may react in several ways: it could be stabilized with a second nucleophilic attack forming the corresponding thioacetal (*C*) after water removal. Another hypothetical pathway is the formation of an α, β -unsaturated sulfide intermediate (*D*) through an elimination process. The final possible product concerns the BME adducts that could form oxathiolane derivatized adducts (*B*), but this possibility is slight given their fast hydrolysis compared to the thioacetal^{51, 52}.

Low in situ stabilization of hemithioacetals. Five equivalents of thiolated molecules (BME and MPA) per M-Unit aldehyde/gem-diol were reacted with a synthesized 2,5-anhydro-D-mannose (M-Unit model) for 72h at pH 1, under inert atmosphere. The relative proportions of the final expected compounds were calculated from LC-MS chromatogram integrations of specific *m/z* values corresponding to both proton and sodium adducts ($[M+H]^+$ and $[M+Na]^+$) within the same run (Table 1). This semi-quantitative evaluation was possible since the expected final products have similar structures and

thus expected similar ionization behaviors. Direct LC-MS analyses (Table 1) of the reaction media (Method I, Figure 4) indicated that the hemithioacetal intermediate *A* corresponded to the major observed compound (75%), the minor product being the stable thioacetal *C* (25%), after 72h reaction. A highly similar 4:1 ratio of hemithioacetal to thioacetal was observed for all thiol models (BME and MPA) tested. Thus the stabilization to the thioacetal intermediate *A* seems to occur with a second thiol nucleophilic attack to form the corresponding thioacetal *C* with the release of water. However, our results suggest that this stabilization occurs only to a relatively low extent in aqueous medium.

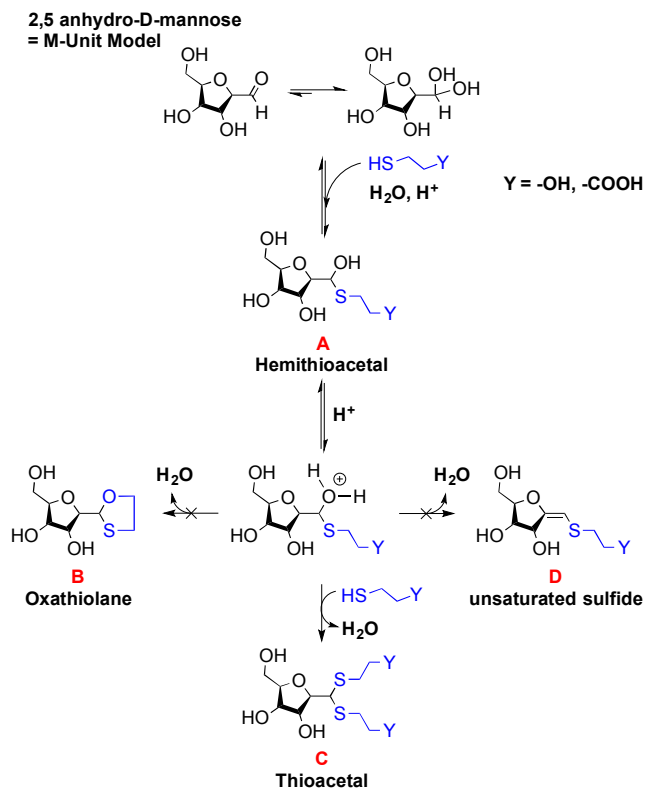


Figure 6. Schematic representation of potential reactions occurring during conjugation of 2,5-anhydro-D-mannose (M-Unit) and 2 thiol-bearing models (3-mercaptopropionic acid and β -mercaptoethanol, MPA and BME respectively) giving the following expected products: Product A is the hemithioacetal intermediate that is in equilibrium with its corresponding oxonium, whereas products B and C correspond to the oxathiolane (for BME reactions only) and thioacetal, respectively. Molecule D represents the α, β -unsaturated sulfide. The results of this study suggest that the thioacetal C corresponds to the only stable form observed after freeze-drying.

Freeze-drying facilitates the hemithioacetal stabilization.

Water removal by freeze-drying (FD) is the key-step in Schiff base formation occurring between CS amines and CS terminal aldehyde²⁰. A similar effect might be at play in the reaction with thiolated species. In order to assess whether or not FD could favor a second thiol nucleophilic attack to stabilize the structure, Method II (Direct FD of the reaction medium, Figure 4) was implemented. This strategy resulted in the synthesis of the thioacetal *C* without any detectable quantity of hemithioacetal *A*, as deduced from LC-MS analysis (). These

trends were also observed using Method III (Increase in pH with 1M acetate buffer pH 4 followed by FD, Figure 4), initially proposed to prevent any CS acid hydrolysis that could occur when this method would be transposed to the polymer CS. Reaction mixtures that were treated this way resulted in a significant increase, when compared to Method I, of the relative proportion of stabilized thioacetal *C* vs. hemithioacetal *A*, corresponding to 96% and 82% thioacetal *C* for BME and MPA respectively (Table 1).

It is worth mentioning that the LC-MS analyses only provide the relative proportion of observed species so that similar results obtained with both Methods II and III do not necessarily corresponds to equivalent absolute conversion rates. For instance, since the hemithioacetal formation equilibrium is pH sensitive³³ (increase in pH is known to displace the equilibrium towards the starting materials), the increased relative proportion of thioacetal *C* observed with Method III vs. Method I could be due to a reduction of the absolute amount of hemithioacetal *A* in the reaction mixture. The conversion degrees or functionalization degrees, are calculated below by ¹H NMR of the purified conjugated polymers.

The oxathiolane *B* and α,β -unsaturated sulfide products *D* appeared as traces in both Methods II and III (Table 1). LC-MS chromatograms revealed the same elution time as for thioacetals *C*, suggesting an in-source decomposition of *B/C* into their respective *D* form. The hypothesis that the oxathiolane *B* was formed within the MS apparatus by the ionization of the thioacetal *C* was confirmed by LC-MS/MS analyses of *C* adduct obtained from the reaction of M-Unit and MPA: the fragmentation of *C* produced compound *D* (data not shown).

These experiments suggest that the oxonium intermediate (which is in equilibrium with the hemithioacetal intermediate) is stable enough to favor the thioacetal formation notwithstanding the unsaturated compound *D* formation. The freeze-drying step apparently orients the reaction towards the stable thioacetal formation, more likely due to an increase in

concentration by water removal to facilitate the second nucleophilic attack.

M-Unit Chitosan HCl salt reactivity

Chitosan HCl salt maintains the M-Unit integrity after freeze-drying. The 2,5-anhydro-D-mannose unit (M-Unit) resulting from CS depolymerization using HONO is not stable after rehydration in aqueous acidic conditions. Indeed, when the reaction medium is neutralized, the reaction between CS amines and the M-Unit aldehyde moiety produces a reversible imino bond (Schiff base formation), which is accompanied with the release of water (Figure 1 – reaction 3). It has been demonstrated that after FD, which is accompanied by Schiff base formation via equilibrium displacement, the solubilization of CS in acidic conditions (pH below 5) cleaves 2,5-anhydro-D-mannose unit from CS into hydroxymethylfurfural (HMF)²⁰ (Figure 1 – reaction 4). In terms of reactivity, the M-Unit is available within the reaction medium after HONO treatment but its concentration is limited to that of the depolymerization medium (0.5% w/v in our case, corresponding to a concentration of reactive units of 2.5 mM for CS with Mn = 2 kg.mol⁻¹). Higher CS depolymerization concentrations are possible (typically up to 2% w/v for CS with Mn of a few hundreds of kg.mol⁻¹) but limited by the high viscosity of CS solutions, which may compromise stirring efficiency and homogeneity of the depolymerization medium. In order to maintain the M-Unit integrity and to work in a more concentrated regime, the depolymerized (i.e. less viscous) CS hydrochloride salt was freeze-dried, with all CS amines protonated, thus avoiding Schiff base formation and subsequent HMF formation upon rehydration. All the CSs that were prepared this way still carried their M-Unit after rehydration (M-Unit remaining $\geq 80\%$), allowing higher CS concentration than the depolymerization medium (4% w/v vs. 0.5% w/v, respectively).

Table 1. Expected product (Figure 6) proportions as deduced from LC-MS analyses. Percentages represent the relative proportion of expected final molecules resulting from each conjugation that were implemented in triplicates ($N \geq 3 \pm SD$): A) Hemithioacetal intermediate, B) Oxathiolane (for β -mercaptoethanol only), C) Thioacetal, D) α,β -unsaturated sulfide. Calculations are based on chromatogram peak integrations of both proton and sodium adducts of a specific chemical formula. m/z given in parentheses represents the thioacetal in-source decomposition observations. Method I refers to direct LC-MS analysis of the reaction medium; Method II corresponds to the direct freeze-drying (FD) of the reaction medium before analysis; Method III corresponds to an increase in pH with acetate buffer pH 4 followed by FD. With both models, the hemithioacetal intermediate is stabilized by FD into the corresponding thioacetal. LC-MS/MS experiments rule out the possible formation (post-FD) of both oxathiolane and α,β -unsaturated sulfide (B and D forms in Figure 6, respectively).

Models	Final product (see Fig. 6)	Chemical Formula	Expected m/z		Observed m/z		Relative proportion (%)		
			[M+H] ⁺	[M+Na] ⁺	[M+H] ⁺	[M+Na] ⁺	Method I	Method II	Method III
M-Unit + BME	A	C8 H16 O6 S	241.0740	263.0560	-	263.0550	75 \pm 13	-	4 \pm 3
	B, D	C8 H14 O5 S	223.0635	245.0454	-	(245.0450)	-	-	-
	C	C10 H20 O6 S2	301.0774	323.0590	301.0884	323.0577	25 \pm 13	100	96 \pm 3
M-Unit + MPA	A	C9 H16 O7 S	269.0689	291.0509	-	291.0502	76 \pm 3	-	18 \pm 7
	C	C12 H20 O8 S2	357.0672	379.0492	-	379.0483	24 \pm 3	100	82 \pm 7
	D	C9 H14 O6 S	251.0584	273.0403	(251.0563)	(273.0386)	-	-	-

The covalent nature of the conjugation of the CS HCl salt M-Unit to thiol-bearing molecules was confirmed by the Ellman assay where no free thiol moieties were detected after rehydration of the modified polymers. Note that free thiol moieties were not detected after Zn/HCl treatment that would have reduced any disulfide bond potentially formed in the course of the conjugation reaction and/or post-reaction workup. The absence of any hemithioacetal intermediate (base sensitive) was also confirmed by performing the Ellman assay on the product after exposure to 1M sodium hydroxide solution. Purified CS-thiol adducts were also analyzed by diffusion ordered spectroscopy (DOSY), a spectroscopic method that

distinguishes compounds according to their respective translation diffusion coefficient (Sup. info. S5), shows that both CS and thiol-bearing models have the same diffusion coefficient in D₂O at 25°C, despite significant molar mass differences (2,300 g.mol⁻¹ vs. 106 g.mol⁻¹, for M-Unit CS HCl salt and MPA respectively). Altogether, the aforementioned controls confirmed the presence of the thioacetal linkage between the CS HCl salt M-Unit and both thiol-bearing model species. The results of the conjugation efficiencies between CS and BME or MPA were calculated using Equation 2 and Equation 3 respectively and are summarized in Table 2.

Table 2. Efficiency of conjugation of the M-Unit CS HCl salt to 5 equivalents of thiol-bearing molecules (3-mercaptopropionic acid and β-mercaptoethanol, MPA and BME respectively) per CS end unit for 72 hours at pH 1. Reaction media were treated according to the following workups: Workup I (Dialysis vs. HCl 1mM solution + FD); Workup II (FD + Dialysis vs. HCl 1mM solution + FD); Workup III (Increase in pH with acetate buffer pH 4 + FD + Dialysis vs. HCl 1mM solution + FD). F below corresponds to the functionalization degree, considering 2 thiol molecules per potential aldehyde and calculated using Equation 2 for BME and Equation 3 for MPA with N≥3 (±SD). F was also calculated using Equation 5, considering only the relative proportion of the remaining gem-diol per M-Unit. (*) corresponds to the results of the conjugations implemented with 20 equivalents (instead of 5) of thiol-bearing molecule per end unit.

Thiol-Bearing Molecules	Temperature (°C)	Workup I		Workup II		Workup III	
		F (%) Eq. 2&3	F (%) Eq. 5	F (%) Eq. 2&3	F (%) Eq. 5	F (%) Eq. 2&3	F (%) Eq. 5
BME	25	2 (±1)	3 (±1)	18 (±2)	18 (±1)	11 (±2)	11 (±1)
	50	26 (±2)	24 (±1)	42 (±2)	42 (±3)	24 (±1)	24 (±0)
		68 (±1) *	69 (±1) *	70 (±1) *	70 (±1) *	-	-
MPA	25	10 (±1)	11 (±1)	18 (±2)	19 (±2)	15 (±1)	13 (±2)
	50	14 (±1)	13 (±1)	54 (±5)	55 (±2)	18 (±1)	17 (±1)
		56 (±1) *	55 (±1) *	59 (±1) *	58 (±1) *	-	-

NMR and LC-MS analyses indicate that two thiol-bearing molecules regioselectively react with CS M-Unit aldehyde to form a thioacetal. The regioselectivity of the CS M-Unit aldehyde conjugation to the thiol models was assessed by 2D NMR experiments (COSY and HMBC, data not shown) in order to detect long-range correlations between the M-Unit and the thiol characteristic peaks. However, such correlations were not visible in the NMR spectra, most probably because of the inherently low concentration of the end-group conjugated thiols within the synthesized structures and/or because the atoms to correlate are separated by a large number of bonds (3 and 4 for proton-carbon and proton-proton correlation, respectively – see Figure 5), especially for the COSY experiments^{53, 54}. Moreover, the HMBC measurements were found to be insensitive, particularly with poorly resolved ¹H-¹H multiplets (Sup. info. S2 and Sup. info. S3)^{55, 56}.

Despite the inability of these 2D NMR experiments to reveal the expected correlations, the combined NMR and LC-MS analysis indicated that two thiol-bearing molecules react regioselectively with the aldehyde of the terminal M-Unit of chitosan. As discussed above, the MS experiments performed with the mannose monomer indicated clearly that the stabilized form is the thioacetal form, so that, two thiols are expected to react similarly with the M-Unit of chitosan. This expected

stoichiometry and regioselectivity for thiol-bearing molecules reacting on chitosan was validated by monitoring the relative proportion of *gem*-diol. Indeed, the *gem*-diol signal should decrease concomitantly with the conjugation of thiols onto the M-Unit of chitosan (one *gem*-diol consumed for two conjugated thiols). The calculated conjugation efficiencies obtained with either Equation 2 (BME) or Equation 3 (MPA) and the following equation should therefore be the same if two thiols react regioselectively onto the terminal aldehyde function of chitosan:

$$F = \frac{\frac{1}{2} \sum \int (H_4M + H_5M) - \int H_{Gem-Diol}}{\frac{1}{2} \sum \int (H_4M + H_5M)} \times 100 \quad \text{Equation 5}$$

Where H₄M and H₅M are protons with well-defined NMR peaks from the M-Unit shown in Figure 5 (unchanged by the reaction of the aldehyde with thiol-bearing molecules) and H_{Gem-Diol} is the H1 proton of the *gem*-diol form of CS M-Unit shown in Sup. info. S1. It is worth mentioning that efficiency calculation using Equation 5 is independent from the reaction stoichiometry and relies only on the assumption that any thiol-bearing molecule will react selectively with the terminal unit of chitosan.

For all conjugation reactions performed in this study, the conjugation efficiencies calculated with both approaches, namely with Equation 2 (BME) or Equation 3 (MPA), which both rely on the reaction stoichiometry, or Equation 5 that is independent from stoichiometry and relies only on the relative proportion of *gem*-diol vs. M-Unit, were found to be in very close agreement (Table 2). These results indicate that 1) thiol-bearing molecules react selectively with the terminal aldehyde functional group of chitosan and 2) the thioacetal is the only stable form of product observed.

The stabilization rate of the product from the hemithioacetal to thioacetal form within the reaction medium can be enhanced by FD. For reactions performed using 5 equivalents of thiol-bearing molecule per aldehyde, the first workup tested here (Workup I: Dialysis vs. HCl 1mM solution + FD), showed a limited conversion into the desired conjugates ($F=2\%$ and 10% as conversion degrees, for BME and MPA at 25°C respectively; Table 2). Similar results were obtained for Workup III (Increase in pH with acetate buffer pH 4 + FD + Dialysis vs. HCl 1mM solution + FD) with $F=11\%$ and 15% at 25°C , for BME and MPA, respectively (Table 2), while significantly higher functionalization degrees were obtained for Workup II (FD + Dialysis vs. HCl 1mM solution + FD) where $F=18\%$ at 25°C , for both BME and MPA (Table 2). Similar trends were observed for reactions performed at 50°C but with an overall increase in functionalization degrees (further discussed in the following section). These results suggest that FD favors the second thiol nucleophilic attack to stabilize the hemithioacetal structure, possibly by concentrating the reaction medium. This FD effect is only seen in Workup II since in Workup I, all thiol-bearing molecules were removed by dialysis prior to FD, while in Workup III, most of the hemithioacetal intermediate was readily transformed into the starting reactants by an increase in pH. Thus, one of the reacting species is absent (or present in very low amount) during the last FD step in Workup I (thiol-bearing molecule removed with concomitant hemithioacetal formation equilibrium displacement towards the starting reactants, Figure 7) and Workup III (hemithioacetal intermediate amount reduced by pH increase) and the thioacetal form cannot be further increased by FD as compared to Workup II where both reacting species are present during FD. In fact, for Workup I and III, all observed thioacetals were mostly formed in situ, during the 72h reaction and results indicate that for reactions performed with 5 equivalents of thiol-bearing molecule per aldehyde, in situ stabilization into the thioacetal form is low.

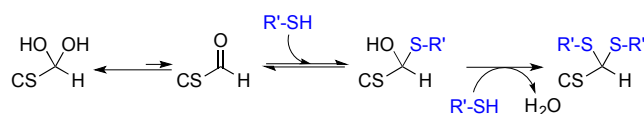


Figure 7. Thiol addition to the aldehyde group of the M-Unit CS HCl salt under acidic aqueous conditions: Despite the fact that the aldehyde is only present in trace amounts within the reaction medium, the pH-dependent hemithioacetal intermediate formation equilibrium can be displaced by the intermediate stabilization into the corresponding thioacetal at low thiol concentration.

Hemithioacetal-to-thioacetal conversion within the reaction medium is increased by large excess of thiol equivalents.

The conjugations implemented with 20 equivalents of thiol-bearing molecules per CS end unit revealed higher conversion rates ($F = 55 - 70\%$ at 50°C depending on the thiol-bearing molecules engaged) and were independent of the workup implemented (i.e. I and II, Table 2). These results also support the proposed reaction mechanism proposed in Figure 7. Indeed, at higher thiol concentrations, hemithioacetal intermediates and thioacetal are both favored within the reaction medium. However, in this case, FD had no significant impact on the conversion degree. Our results suggest that at high thiol concentration (20 equivalents per aldehyde) the amount of thiol-bearing molecules is sufficient to achieve significant hemithioacetal stabilization in situ. The fact that FD has no significant impact on the functionalization rate is unclear and would require additional investigations.

Temperature favors both hemithioacetal formation and stabilization to the thioacetal form.

The highest conversion degrees were obtained at 50°C , regardless of the workup implemented (Table 2). Indeed, an increase in temperature favors the hemithioacetal intermediate formation by increasing the probability of thiol-bearing molecules to react with the CS HCl salt M-Unit aldehyde. Similarly, stabilization of the hemithioacetal intermediate occurred with an increase in temperature, favoring the second thiol model attack by increasing the probability of collisions between species. This mechanism is especially valid for the results corresponding to Workups I and III where no FD stabilization was reported. Indeed, the functionalization degree varied from 2% to 26% for BME and from 10% to 14% for MPA, for 25 and 50°C respectively. The proposed mechanism involving an equilibrium between the starting reactants and the hemithioacetal intermediate (Figure 7) is thus confirmed by this increase in conversion degree with temperature.

Effective CS PEGylation by thioacetylation of the CS M-Unit aldehyde

CS-b-PEG₂ block-copolymer synthesis. As a direct application of the thioacetylation conjugation developed in the paper herein, a 2 kDa mPEG-SH was reacted with a 10 kDa CS HCl salt. The choice of a 2 kDa PEG was based on the CS and PEG molecular weight (M_w) ratio (10 kDa and 2×2 kDa, respectively), expecting the PEG M_w to be large enough to form micellar structures (See section below). Because of solubility limitations with these longer chains, the reaction was performed at 5 mM aldehyde instead of 20 mM that was used for the reactions between the 2 kDa CS and MPA or BME. In order to counterbalance the decrease in aldehyde concentration, the reaction was performed at 50°C for 72h and ten thiol equivalents per aldehyde were used. After direct FD of the reaction medium and unreacted mPEG-SH removal by multiple precipitations, ^1H NMR analysis of the final product (Figure 8) was performed and functionalization degree values (F) of 61% and 51% were found with Equation 4 and Equation 5 (where

only the gem-diol peak integration decrease was considered), respectively.

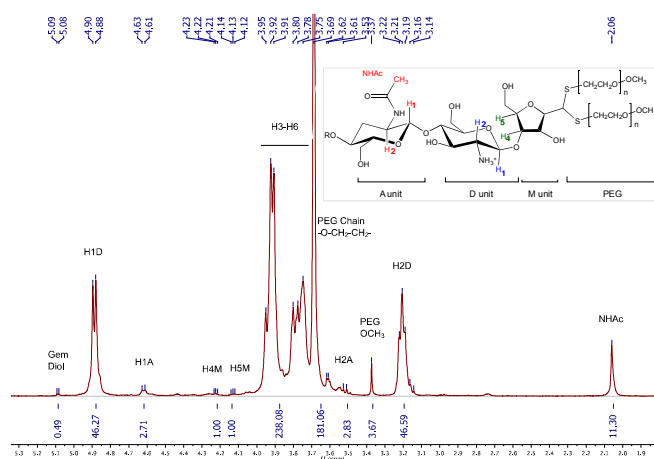


Figure 8. ^1H NMR spectrum of the CS-b-PEG₂ block-copolymer after workup II (D₂O, T=70°C, HOD peak was presaturated, number of scans (ns) = 64, relaxation period (d1) = 6s, Acquisition time=2s, Exponential apodization = 1 Hz). Integration of *Gem*-diol proton peak was used to calculate the functionalization degree (in this particular case, F=51% according to Equation 5).

The slight discrepancy between these two values could possibly be due to the presence of residual mPEG-SH post-purification. This hypothesis was confirmed by SEC analysis of the conjugates, where a small residual peak identified as mPEG-SS-PEGm was detected. Because PEG and CS molecular weights are close to each other, the DOSY NMR processing used to validate covalent conjugation of MPA and BME to CS was found to be inefficient for the block-copolymer (data not shown).

CS-b-PEG₂ block-copolymer/pDNA polyplexes are homogeneously spherical. The CS-b-PEG₂ block-copolymer (CS 92-10 and 2 kDa mPEG-SH) synthesized above was used without further purification to form polyplexes with plasmid DNA (pEGFP_{Luc}). Whereas ESEM imaging of polyplexes prepared with unmodified CS revealed various morphologies, namely toroids, spheres and rods, those prepared with CS-b-PEG₂ block-copolymer were uniformly spherical (Figure 9). The structure modification of the polyplexes formed with PEGylated CS was also confirmed by DLS, where measured Z-average diameters decreased from 106 (±1) nm to 76 (±1) nm, for unmodified CS and CS-b-PEG₂ block-copolymer, respectively (Table 3).

Since the PEGylated polyplexes are uniformly spherical and show a narrower size as compared to those prepared with corresponding homopolyions, these observations are consistent with the formation of micellar structures called “Block Ionomer Complexes” (BICs)⁵⁷⁻⁵⁹.

Table 3. DLS measurements of unmodified CS and CS-b-PEG₂ polyplexes prepared with pDNA (pEGFP_{Luc}, N/P=3.7). Samples were analyzed in triplicates (N=2, ±(max-min)/2). The size of CS-b-PEG₂ polyplexes is smaller as compared to native polyplexes.

Samples	Z-Average diameter (nm)	PDI	Intensity-weighted mean diameter (nm)
Unmodified CS polyplexes	106 (±8)	0.19 (±0.00)	131 (±11)
CS-b-PEG ₂ polyplexes	76 (±5)	0.23 (±0.02)	96 (±11)

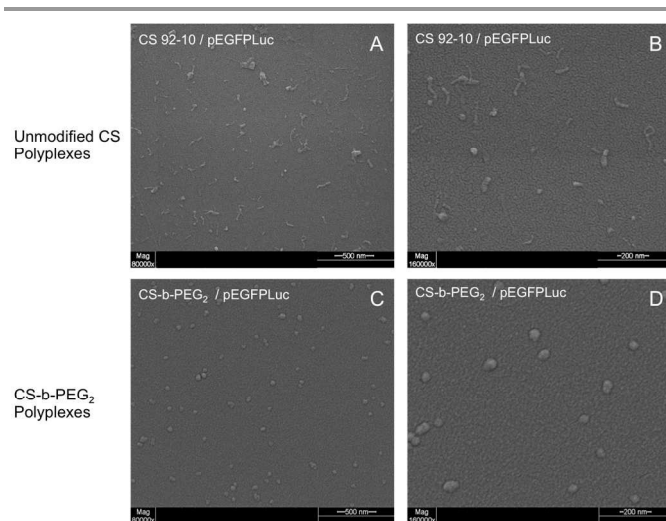


Figure 9. Environmental Scanning Electron Microscopy (ESEM) pictures (High vacuum mode, accelerating voltage = 20.0 kV; spot size = 3 and working distance = 5mm) of polyplexes formed with pDNA and unmodified CS or CS-b-PEG₂ block-copolymer (amine to phosphate ratio = 3.7, N/P=3.7). A & B (x80000 and x160000, respectively): polyplexes formed with CS 92-10 are heterogeneous in size and present various morphologies (globular, rod-like and toroidal). Pictures C and D (x80000 and x160000, respectively): polyplexes formed with CS-b-PEG₂ (CS 92-10 and mPEG-SH 2kDa), are uniformly spherical.

Conclusions

This study revealed that the aldehyde present on chitosan mannose (M-Unit) end group is displaced completely towards its hydrated and unreactive form (*gem*-diol) in aqueous conditions. The ubiquity of the unreactive *gem*-diol form in aqueous conditions revealed by ^1H NMR (dehydrated reactive form not detected) could be due to both H-bonding and hydration effects. Despite the fact that the aldehyde reactive moiety is only present in trace amounts, the development and optimization of a thiol-based chemistry allowed efficient conjugation to the CS terminal M-Unit in aqueous conditions (F = 55 -70% depending on the thiol-bearing molecule). A combination of mass spectrometry and NMR analyses revealed that two thiol-bearing molecules react regioselectively with the terminal aldehyde of the polymer to form a thioacetal. The stabilization of the hemithioacetal intermediate was found to be facilitated by freeze-drying (Figure 10). As a direct application of this novel conjugation strategy, a CS-b-PEG₂ block-copolymer was successfully synthesized by thioacetylation of

the CS 92-10 M-Unit aldehyde with a 2 kDa mPEG-SH. This block-copolymer was used to prepare polyplexes with pDNA

that were found to be uniformly spherical and more homogeneous as compared to those prepared with native CS.

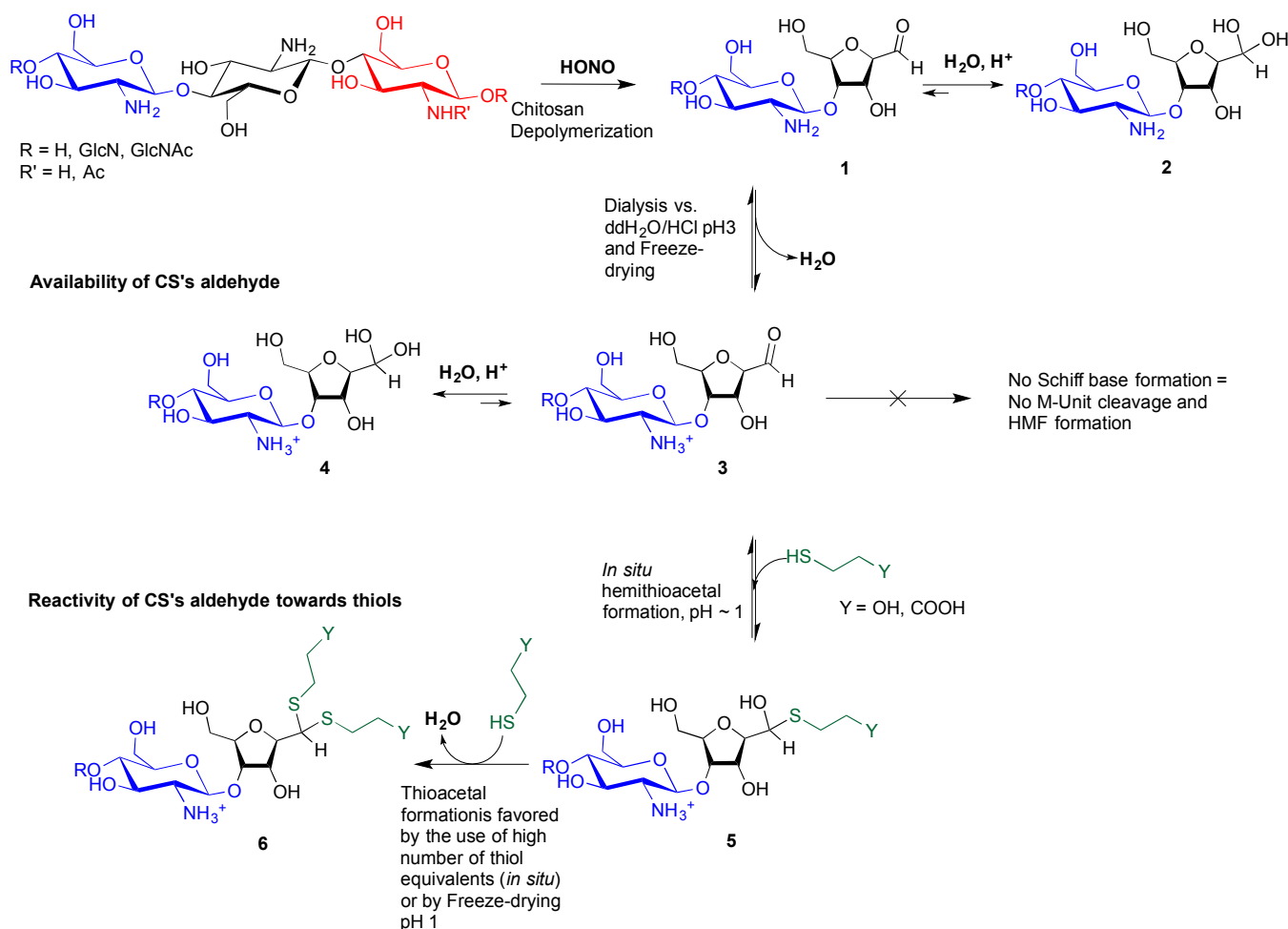


Figure 10. Summary of mechanisms elucidated in this study for thiol-based end-group derivatization of chitosans: CS nitrous acid depolymerization induces the formation of M-Unit that carries an aldehyde moiety at the end of the cleaved polymer (1). The equilibrium between the M-Unit aldehyde and its hydrated form (*gem*-diol) is strongly displaced towards the latter (2). If the CS depolymerization medium is freeze-dried at pH well below the CS pKa (i.e. pH ~3-4 or below), all the CS amines are protonated and are therefore unable to react with any aldehyde group, maintaining the CS M-Unit integrity at the end of the cleaved polymer (3). Nevertheless, the equilibrium between the M-Unit aldehyde and the corresponding *gem*-diol is still displaced towards the hydrated form (4). Despite the undetectable aldehyde moieties, thiol molecules and the M-Unit CS aldehyde are engaged in a pH dependent equilibrium with the corresponding hemithioacetal intermediate (5). The stabilization of the latter into its thioacetal form (6) occurs either by increasing the amount of thiol-bearing reactants in the medium (*in situ* stabilization), or by freeze-drying the reaction medium when low amounts of thiol are engaged.

The new CS end-group thioacetylation process that was developed in this study presents several advantages in comparison to the oxime click method developed previously^{16, 18, 24}. That is 1) it can be used for CS derivatization without interfering with amine groups that are fully protonated and thus unreactive, 2) it is efficient in aqueous media and 3) there is no need for an external chemical treatment to stabilize the adducts. It is worth mentioning that the stabilization of the hemithioacetal intermediate by a second nucleophilic attack could be sterically hindered by the presence of the first external group for large thiol-bearing substituents. In order to circumvent this issue and to further improve the conjugation efficiency, studies are ongoing where a molecule bearing two

thiol groups (a thiol-based “hook”) is used for conjugation to the CS M-Unit. The presence of two thiol moieties along with their adequate positioning on the molecule to be conjugated may allow for an intramolecular stabilization of the hemithioacetal, which is expected to rule out any steric hindrance issues and to occur *in situ* at significantly lower thiol concentrations vs. the intermolecular stabilization studied herein.

CS end-group modifications such as PEGylation and the formation of other types of block-copolymers as well as CS grafting onto surfaces via a single covalent bond are a few applications of our proposed green chemistry protocol. These could be advantageously applied to various biomedical research

fields including gene delivery and tissue engineering. Additionally, we expect this thiol-based chemistry to be applicable to other polymers bearing aldehydes or ketones.

Acknowledgements

This work was supported by the Natural Sciences and Engineering Research Council of Canada (NSERC) and ANRis Pharmaceuticals. The authors would like to acknowledge Monica Ilescu Nelea (Polytechnique Montréal), Alexandra Furtos (Université de Montréal) and Cédric Malveau (Université de Montréal) for the ESEM pictures and helpful discussions on mass spectrometry and NMR spectroscopy, respectively.

Notes and references

^a Dept. Chemical Engineering and Inst. Biomedical Engineering, Ecole Polytechnique, Montreal, QC, Canada

^b ANRis Pharmaceuticals Inc., Kirkland, QC, Canada

† Corresponding authors (marc.lavertu@polymtl.ca and michael.buschmann@polymtl.ca)

Electronic Supplementary Information (ESI) available: [details of any supplementary information available should be included here]. See DOI: 10.1039/b000000x/

- M. Rinaudo, *Progress in Polymer Science*, 2006, **31**, 603-632.
- H. Sashiwa and S.-i. Aiba, *Progress in Polymer Science*, 2004, **29**, 887-908.
- I. Aranaz, R. Harris and A. Heras, *Current Organic Chemistry*, 2010, **14**, 308-330.
- L. Casettari, D. Vllasaliu, E. Castagnino, S. Stolnik, S. Howdle and L. Illum, *Progress in Polymer Science*, 2012, **37**, 659-685.
- M. Garcia-Fuentes and M. J. Alonso, *Journal of controlled release : official journal of the Controlled Release Society*, 2012, **161**, 496-504.
- M. D. Buschmann, A. Merzouki, M. Lavertu, M. Thibault, M. Jean and V. Darras, *Advanced Drug Delivery Reviews*, 2013, **65**, 1234-1270.
- I. K. Park, T. H. Kim, Y. H. Park, B. A. Shin, E. S. Choi, E. H. Chowdhury, T. Akaike and C. S. Cho, *Journal of Controlled Release*, 2001, **76**, 349-362.
- O. Germershaus, S. Mao, J. Sitterberg, U. Bakowsky and T. Kissel, *Journal of Controlled Release*, 2008, **125**, 145-154.
- C. Zhang, Q. Ping, Y. Ding, Y. Cheng and J. Shen, *Journal of Applied Polymer Science*, 2004, **91**, 659-665.
- J. You, F. Q. Hu, Y. Z. Du and H. Yuan, *Biomacromolecules*, 2007, **8**, 2450-2456.
- J. H. Na, H. Koo, S. Lee, K. H. Min, K. Park, H. Yoo, S. H. Lee, J. H. Park, I. C. Kwon, S. Y. Jeong and K. Kim, *Biomaterials*, 2011, **32**, 5252-5261.
- H. Prichystalova, N. Almonasy, A. M. Abdel-Mohsen, R. M. Abdel-Rahman, M. M. Fouda, L. Vojtova, L. Kobera, Z. Spotz, L. Burgert and J. Jancar, *International journal of biological macromolecules*, 2014, **65**, 234-240.
- F. Lebouc, I. Dez, J. Desbrières, L. Picton and P.-J. Madec, *Polymer*, 2005, **46**, 639-651.
- K. Tommerraas, M. Koping-Hoggard, K. M. Varum, B. E. Christensen, P. Artursson and O. Smidsrod, *Carbohydrate research*, 2002, **337**, 2455-2462.
- M. Morimoto, M. Nakao, N. Ishibashi, Y. Shigemasa, S. Ifuku and H. Saimoto, *Carbohydrate Polymers*, 2011, **84**, 727-731.
- US Pat.*, 2012.
- S. K. Tripathi, R. Goyal, M. P. Kashyap, A. B. Pant, W. Haq, P. Kumar and K. C. Gupta, *Biomaterials*, 2012, **33**, 4204-4219.
- B. E. Benediktsdottir, K. K. Sorensen, M. B. Thygesen, K. J. Jensen, T. Gudjonsson, O. Baldursson and M. Masson, *Carbohydr Polym*, 2012, **90**, 1273-1280.
- J. M. Los, L. B. Simpson and K. Wiesner, *Journal of the American Chemical Society*, 1956, **78**, 1564-1568.
- K. Tommerraas, K. M. Vårum, B. E. Christensen and O. Smidsrod, *Carbohydrate research*, 2001, **333**, 137-144.
- E. P. Azevedo, S. V. Santhana Mariappan and V. Kumar, *Carbohydrate Polymers*, 2012, **87**, 1925-1932.
- G. G. Allan and M. Peyron, *Carbohydrate research*, 1995, **277**, 257-272.
- D. Filion, M. Lavertu and M. D. Buschmann, *Biomacromolecules*, 2007, **8**, 3224-3234.
- R. Novoa-Carballal and A. H. E. Muller, *Chemical Communications*, 2012, **48**, 3781-3783.
- R. Novoa-Carballal, C. Silva, S. Moller, M. Schnabelrauch, R. L. Reis and I. Pashkuleva, *Journal of Materials Chemistry B*, 2014, **2**, 4177-4184.
- T. O. Eloranta, A. R. Khomutov, R. M. Khomutov and T. Hyvonen, *Journal of biochemistry*, 1990, **108**, 593-598.
- J. Kalia and R. T. Raines, *Angewandte Chemie International Edition*, 2008, **47**, 7523-7526.
- T. S. Zatsepin, D. A. Stetsenko, A. A. Arzumanov, E. A. Romanova, M. J. Gait and T. S. Oretskaya, *Bioconjugate chemistry*, 2002, **13**, 822-830.
- J. Shao and J. P. Tam, *Journal of the American Chemical Society*, 1995, **117**, 3893-3899.
- G. E. Lienhard and W. P. Jencks, *Journal of the American Chemical Society*, 1966, **88**, 3982-3995.
- E. G. Sander and W. P. Jencks, *Journal of the American Chemical Society*, 1968, **90**, 6154-6162.
- M. P. Schubert, *Journal of Biological Chemistry*, 1936, **114**, 341-350.
- R. E. Barnett and W. P. Jencks, *Journal of the American Chemical Society*, 1967, **89**, 5963-5964.
- R. Caraballo, H. Dong, J. P. Ribeiro, J. Jiménez-Barbero and O. Ramström, *Angewandte Chemie*, 2010, **122**, 599-603.
- E. Campaigne, in *Organic Sulfur Compounds*, ed. N. Kharasch, Pergamon, 1961, pp. 134-145.
- T. W. G. Peter G. M. Wuts, in *Protective groups in organic synthesis*, ed. Wiley, 2006, ch. 4, pp. 477-500.
- R. Lumry, E. L. Smith and R. R. Glantz, *Journal of the American Chemical Society*, 1951, **73**, 4330-4340.
- S. Clause, F. Bringaud, L. Azéma, R. Baron, J. Périé and M. Willson, *Carbohydrate research*, 1999, **315**, 339-344.
- M. Erlandsson and M. Hällbrink, *Int J Pept Res Ther*, 2005, **11**, 261-265.
- M. Lavertu, Z. Xia, A. N. Serreji, M. Berrada, A. Rodrigues, D. Wang, M. D. Buschmann and A. Gupta, *Journal of Pharmaceutical and Biomedical Analysis*, 2003, **32**, 1149-1158.
- M. Lavertu, V. Darras and M. D. Buschmann, *Carbohydrate Polymers*, 2012, **87**, 1192-1198.
- S. Nguyen, F. M. Winnik and M. D. Buschmann, *Carbohydrate Polymers*, 2009, **75**, 528-533.
- D. Banfi and L. Patiny, *Chimia*, 2008, **62**, 280-281.
- M. Lavertu, S. Méthot, N. Tran-Khanh and M. D. Buschmann, *Biomaterials*, 2006, **27**, 4815-4824.
- Y. Niebel, M. D. Buschmann, M. Lavertu and G. De Crescenzo, *Biomacromolecules*, 2014, **15**, 940-947.
- R. Bell, *Adv. Phys. Org. Chem.*, 1966, **4**, 1-29.
- L. Heux, J. Brugnerotto, J. Desbrières, M. F. Versali and M. Rinaudo, *Biomacromolecules*, 2000, **1**, 746-751.
- J. L. Axson, K. Takahashi, D. O. De Haan and V. Vaida, *Proceedings of the National Academy of Sciences*, 2010, **107**, 6687-6692.
- H. Saito, R. Tabeta and K. Ogawa, *Macromolecules*, 1987, **20**, 2424-2430.
- E. M. Schulman, O. D. Bonner, D. R. Schulman and F. M. Laskovics, *Journal of the American Chemical Society*, 1976, **98**, 3793-3799.

51. D. P. N. Satchell and R. S. Satchell, *Chemical Society Reviews*, 1990, **19**, 55-81.
52. L. Fournier, G. Lamaty, A. Natat and J. P. Roque, *Tetrahedron*, 1975, **31**, 1025-1029.
53. T. D. Claridge, *High-resolution NMR techniques in organic chemistry*, Newnes, 2008.
54. D. Pinto, C. M. Santos and A. M. Silva, *Recent Research Developments in Heterocyclic Chemistry, Pinho e Melo, Research Signpost, Kerala (India)*, 2007.
55. A. Bax, K. A. Farley and G. S. Walker, *Journal of Magnetic Resonance, Series A*, 1996, **119**, 134-138.
56. J. Furrer, *Chemical Communications*, 2010, **46**, 3396-3398.
57. A. V. Kabanov and V. A. Kabanov, *Bioconjugate chemistry*, 1995, **6**, 7-20.
58. I. K. Voets, A. de Keizer and M. A. Cohen Stuart, *Advances in Colloid and Interface Science*, 2009, **147-148**, 300-318.
59. D. V. Pergushov, A. H. E. Muller and F. H. Schacher, *Chemical Society Reviews*, 2012, **41**, 6888-6901.